

## EVIDENCE FOR A YOUNG STELLAR POPULATION IN NEARBY TYPE 1 ACTIVE GALAXIES

MINJIN KIM<sup>1,2</sup> AND LUIS C. HO<sup>3,4</sup>*Draft version March 22, 2019*

## ABSTRACT

To understand the physical origin of the close connection between supermassive black holes and their host galaxies, it is vital to investigate star formation properties in active galaxies. Using a large dataset of nearby type 1 active galactic nuclei (AGNs) with detailed structural decomposition based on high-resolution optical images obtained with the *Hubble Space Telescope*, we study the correlation between black hole mass and bulge luminosity and the (Kormendy) relation between bulge effective radius and surface brightness. In both relations, the bulges of type 1 AGNs tend to be more luminous than those of inactive galaxies with the same black hole mass or the same bulge size. This suggests that the central regions of AGN host galaxies have characteristically lower mass-to-light ratios than inactive galaxies, most likely due to the presence of a younger stellar population in active systems. In addition, the degree of luminosity excess appears to be proportional to the accretion rate of the AGN, revealing a physical connection between stellar growth and black hole growth. Adopting a simple toy model for the increase of stellar mass and black hole mass, we show that the fraction of young stellar population flattens out toward high accretion rates, possibly reflecting the influence of AGN-driven feedback.

**Keywords:** galaxies: active — galaxies: bulges — galaxies: fundamental parameters — galaxies: photometry — quasars: general

## 1. INTRODUCTION

Star formation in galaxies is often thought to be closely linked with black hole (BH) growth, as inferred from the observed correlation between BH mass and the stellar mass of the host galaxy bulge (Magorrian et al. 1998; Kormendy & Ho 2013). As active galactic nuclei (AGNs) signify rapid BH growth, strong star formation should occur in AGN host galaxies. However, AGN activity and star formation occur on different timescales, and there is still considerable debate as to whether stellar growth and black hole growth are synchronized (e.g., Hickox et al. 2014).

Previous observational studies have shown diverse results on the connection between stellar growth and BH growth. Studying star formation in AGN host galaxies is challenging because the majority of the traditional star formation rate (SFR) indicators (UV, H $\alpha$ , mid-infrared emission) can be heavily contaminated by the AGN itself. Far-infrared (FIR) emission has been widely used to estimate SFR in AGN hosts, as the FIR emission from cold dust is thought to be dominated by star formation rather than AGNs. Earlier FIR studies of nearby luminous AGNs showed that SFR appears to be tightly correlated with BH accretion rate (e.g., Netzer 2009). However, more recent investigations, mostly based on *Herschel* observations, reveal that AGNs with moderate to low luminosity tend to have moderate SFRs regardless of the AGN luminosity, revealing a weak connection between star formation and BH growth (e.g., Mullaney et al. 2012; Rosario et al. 2012, 2015). One of the main limitations of these studies is that FIR emission itself can originate from cold dust heated by the AGN (e.g., Symeonidis et al. 2016; Symeonidis 2017;

Shangguan et al. 2018). The FIR luminosity can overestimate the SFR in AGN hosts if the contribution from the AGN is not properly taken into account. Some investigators make use of the mid-infrared emission from polycyclic aromatic hydrocarbons to trace star formation (e.g., Shi et al. 2007; Shipley et al. 2013; Alonso-Herrero et al. 2014), but there are lingering doubts as to the extent to which these molecules are destroyed in AGN environments (e.g., O’Dowd et al. 2009).

Ho (2005) proposed that, as in normal galaxies, the luminosity of [O II]  $\lambda 3727$  can be used to constrain the SFR in active galaxies. Contrary to the results based on FIR observations, studies using [O II] emission as a SFR indicator find that star formation tends to be moderately weak in nearby type 1 (unobscured, broad-line) AGNs, regardless of their AGN luminosity (Kim et al. 2006), while star formation is enhanced in either distant type 1 or luminous type 2 (obscured, narrow-line) AGNs (Silverman et al. 2008; Kim et al. 2006). However, dust extinction presents a potential source of uncertainty for [O II] emission; SFRs computed from [O II] can be systematically underestimated if star formation occurs mainly in dust-enshrouded regions.

In light of the above-mentioned technical difficulties to constrain *ongoing* star formation in AGNs, a useful alternative strategy is to investigate *recent* star formation activity in AGN host galaxies. Analyzing the optical stellar continuum of spectra selected from the Sloan Digital Sky Survey, Kauffmann et al. (2003) found evidence for a young (ages  $\sim 10^8$  yr) stellar population in moderate-luminosity type 2 AGNs. They argued that the fraction of young stars appears to be proportional to the strength (luminosity) of the AGN, suggesting a close connection between stellar growth and BH growth. On the other hand, AGN host galaxies appear to have a wide range of colors. Several studies show that galaxies with moderate-luminosity AGNs tend to have colors intermediate between those of red quiescent galaxies and blue star-forming galaxies (Silverman et al. 2008; Schawinski et al. 2009; Rosario et al. 2013), again revealing enhanced recent star formation in AGN hosts. By contrast,

<sup>1</sup> Department of Astronomy and Atmospheric Sciences, Kyungpook National University, Daegu 702-701, Korea; mkim.astro@gmail.com

<sup>2</sup> Korea Astronomy and Space Science Institute, Daejeon 305-348, Korea

<sup>3</sup> Kavli Institute for Astronomy and Astrophysics, Peking University, Beijing 100871, China; lho.pku@gmail.com

<sup>4</sup> Department of Astronomy, School of Physics, Peking University, Beijing 100871, China

other studies report that the rest-frame optical colors of the host galaxies of moderate-luminosity AGNs are consistent with those of inactive galaxies (e.g., Cardamone et al. 2010; Bruce et al. 2016), as has been known to be the case for low-luminosity AGNs (Ho et al. 2003).

Notwithstanding these many previous attempts, it is still vital to better understand the recent star formation history of luminous type 1 AGNs, the phase during which BHs gain significant mass. With the advent of empirical methods to calculate BH masses for type 1 AGNs using single-epoch spectra (e.g., Kaspi et al. 2000), in combination with bolometric corrections to estimate bolometric luminosities (e.g., McLure & Dunlop 2004; Krawczyk et al. 2013), the specific BH growth rate, defined as the mass accretion rate divided by BH mass, can be easily inferred. Decomposing the photometric properties of the host galaxies of type 1 AGNs remains a technical challenge because the bright active nucleus often overwhelms and substantially contaminates the stellar signal. Thus, previous studies of the host galaxies of type 1 AGNs have been conducted with heterogeneous, limited samples and have reached diverse conclusions regarding their stellar population. Some (Sánchez et al. 2004; Canalizo & Stockton 2013; Matsuoka et al. 2014) find that the host galaxies of luminous type 1 AGNs have bluer colors than normal galaxies of similar stellar mass, indicating recently enhanced star formation, while others (e.g., Nolan et al. 2001; Bettoni et al. 2015) disagree.

In this paper, we investigate the stellar population in nearby type 1 AGNs using the photometric properties of their host galaxies derived from *Hubble Space Telescope* (*HST*) images analyzed in Kim et al. (2017). We employ two independent methods—the empirical  $M_{\text{BH}} - L_{\text{bul}}$  relation and the Kormendy relation—to demonstrate that AGN hosts are over-luminous with respect to normal, inactive galaxies, an effect we attribute enhanced recent star formation. The sample and data are presented in Section 2. We describe the scaling relations in Section 3. We discuss the implications of the results in Section 4 and summarize our findings in Section 5. This work adopts the Vega magnitude system (Bessell 2005) and the cosmological parameters  $H_0 = 100h = 67.8 \text{ km s}^{-1} \text{ Mpc}^{-1}$ ,  $\Omega_m = 0.308$ , and  $\Omega_\Lambda = 0.692$  (Planck Collaboration et al. 2016).

## 2. DATA

The sample and image analysis are described in detail in Kim et al. (2017). We select type 1 AGNs that have suitable optical images in the *HST* archive as well as spectroscopic data either from the literature or from our own observations (Ho & Kim 2009) of sufficient quality to enable their BH masses to be estimated (see Section 2.2). All photometric quantities have been transformed to the *R* band. We only choose nearby objects with  $z < 0.35$  in order to minimize evolutionary effects. Our sample includes 235 objects, spanning a wide diversity of properties, from traditional broad-line Seyfert 1s and quasars to narrow-line Seyfert 1s, radio-loud and radio-quiet. In addition to the sample from Kim et al. (2017), we expand the dynamic range in physical properties by including the sample of 132 low-mass AGNs ( $M_{\text{BH}} \leq 10^{6.3} M_\odot$ ) from Jiang et al. (2011). Since Jiang et al. (2011) analyzed *I*-band (F814W) images, we convert their *I*-band photometry to *R* band assuming  $R - I = 0.65 \text{ mag}$  from Fukugita et al. (1995), appropriate for Sbc galaxies. In total, we use a sample of 367 type 1 AGNs in this study.

### 2.1. Host Properties

We performed two-dimensional imaging analysis using GALFIT v3.0 (Peng et al. 2002, 2010). GALFIT allows us to decompose the central nucleus from the host galaxy, which is modeled with a bulge, and, if necessary, a disk and a bar. The galaxy components are modeled with Fourier modes to accommodate complex, non-axisymmetric features such as tidal distortions or spiral arms. We have also performed comprehensive and extensive simulations to understand the measurement errors in the decomposition (Kim et al. 2008a). We find that the luminosity ratio of the nucleus to the underlying bulge is the main factor that determines the uncertainty of the bulge luminosity. The uncertainty can increase when decomposition of bulge and disk is required, or when the central core of the image is saturated. Typical uncertainties of the bulge luminosity range from 0.4 to 0.7 mag. *K*-correction and color conversion from the observed filters to the *R*-band filter employ galaxy templates from Calzetti et al. (1994) and Kinney et al. (1996). It is difficult to perform visual classification of the morphology of the host galaxies because the light is often overwhelmed by the bright nucleus. Instead, we use the measured bulge-to-total light ratio ( $B/T$ ) and an empirical correlation between  $B/T$  and Hubble type (Gao et al. 2019) to determine the morphological type of the hosts.

Although our sample is relatively nearby, the bulge brightness can be affected by passive luminosity evolution, in the sense that more distant hosts are naturally more luminous because of younger stellar population. In order to take into account this luminosity evolution, we adopt  $dM_R/dz \approx -0.73$ , derived from a simple starburst model (Treu et al. 2002; Peng et al. 2006; Kim et al. 2017). This correction, however, barely affects the final conclusions of this paper.

### 2.2. Black Hole Masses

We derive BH masses using the empirical BH estimator for single-epoch spectra:

$$\log(M_{\text{BH}}/M_\odot) = a + 0.533 \log \left( \frac{L_{5100}}{10^{44} \text{ erg s}^{-1}} \right) + 2 \log \left( \frac{\text{FWHM}}{10^3 \text{ km s}^{-1}} \right), \quad (1)$$

where FWHM refers to the width of the broad  $\text{H}\beta$  line,  $L_{5100}$  is the AGN continuum luminosity at  $5100 \text{ \AA}$  estimated from the nucleus magnitude obtained from the *HST* image decomposition (Kim et al. 2017), and  $a = (7.03, 6.62, 6.91)$  for classical bulges and ellipticals, pseudo bulges, and all bulge types combined, respectively (Ho & Kim 2015). The different normalizations take into account the bulge type-dependent virial coefficient (Ho & Kim 2014), which reflects the fact that the  $M_{\text{BH}} - \sigma_*$  relation of inactive galaxies differs between classical and pseudo bulges (Kormendy & Ho 2013). Whenever possible, Kim et al. (2017) classified the bulges of the AGN hosts using the Sérsic index and bulge-to-total light ratio [classical bulges ( $n > 2$  and  $B/T > 0.2$ ) and pseudo bulges ( $n \leq 2$  or  $B/T \leq 0.2$ )]. The bulges of some objects could not be classified because of the ambiguity of their photometric fits (e.g., merging features and dust lanes). For the sample from Jiang et al. (2011), galaxies with  $B/T \leq 0.2$  are deemed to host pseudo bulges.

The error budget for the BH mass mostly comes from the uncertainty in the virial factor ( $\sim 0.4 \text{ dex}$ ; Onken et al. 2004;

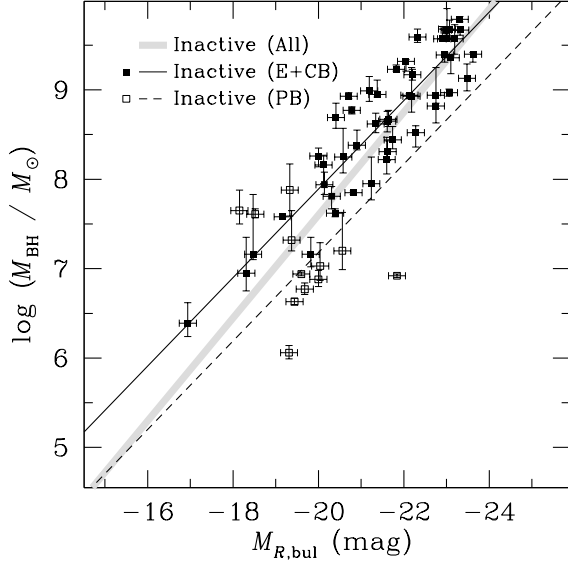


**Figure 1.** Correlation between BH mass and absolute  $R$ -band magnitude for inactive galaxies. Shaded grey line represents the relation for inactive galaxies, including ellipticals, classical bulges, and pseudo bulges, adapted from Kormendy & Ho (2013). Filled squares and solid line denote ellipticals and classical bulges and their relation; open circles and dashed line denote pseudo bulges and their relation.

Collin et al. 2006; Woo et al. 2010; Ho & Kim 2014). Taking into account additional factors contributing to the uncertainty (e.g., measurement error on FWHM, intrinsic scatter of the broad-line region size-luminosity relation, and AGN variability), we conservatively adopt 0.5 dex for the uncertainty for the BH masses. We estimate the bolometric luminosity and Eddington ratio ( $\lambda_E \equiv L_{\text{bol}}/L_{\text{Edd}}$ ) using a bolometric correction of  $L_{\text{bol}} = 9.8L_{5100}$  (McLure & Dunlop 2004).

### 3. SCALING RELATIONS

#### 3.1. $M_{\text{BH}}-L_{\text{bul}}$ Relation

To enable comparison between active and inactive galaxies, we first derive the  $M_{\text{BH}}-L_{\text{bul}}$  relation of inactive galaxies in the  $R$  band, using the sample and data from Kormendy & Ho (2013). To convert bulge stellar mass to  $R$ -band luminosity, we use a mass-to-light ratio calculated from the  $B-V$  colors of the bulges of the individual galaxies (Into & Portinari 2013). We then fit a linear relation of the form

$$\log(M_{\text{BH}}/M_{\odot}) = \alpha + \beta M_{R,\text{bul}}. \quad (2)$$

The fitting procedure adopts the  $\chi^2$ -minimization method of Tremaine et al. (2002), which takes into account errors in both parameters. To account for an intrinsic scatter ( $\epsilon_0$ ) in the  $M_{\text{BH}}-L_{\text{bul}}$  relation,  $\chi^2$  is written as

$$\chi^2 = \frac{y_i - (\alpha + \beta x_i)}{\epsilon_0^2 + \sigma_{y,i} + \beta \sigma_{x,i}}, \quad (3)$$

where  $y_i = \log(M_{\text{BH}}/M_{\odot})$ ,  $x_i = M_{R,\text{bul}}$ , and  $\sigma_{y,i}$  and  $\sigma_{x,i}$  are measurement errors of  $y_i$  and  $x_i$ , respectively. The best-fit parameters for inactive galaxies are  $\alpha = -3.92 \pm 0.82$ ,  $\beta = -0.58 \pm 0.04$  and  $\epsilon_0 = 0.53 \pm 0.06$ .

Kormendy & Ho (2013) argue that the BH-host scaling relations depend on bulge type. To account for this effect, we derive the  $M_{\text{BH}}-L_{\text{bul}}$  relations for two subsamples according

Table 1.  $M_{\text{BH}}-M_{R,\text{bul}}$  Relation for Different Subsamples.

Subsamples (1)	$\alpha$ (2)	$\beta$ (3)	$\epsilon_0$ (4)
Inactive (All)	$-3.92 \pm 0.82$	$-0.58 \pm 0.04$	$0.53 \pm 0.06$
AGNs (All)	$-4.56 \pm 0.04$	$-0.58^a$	$0.40 \pm 0.04$
AGNs (All)	$-2.27 \pm 0.40$	$-0.46 \pm 0.02$	$0.36 \pm 0.04$
AGNs (All; $\lambda_E \leq 0.1$ )	$-4.32 \pm 0.06$	$-0.58^a$	$0.39 \pm 0.07$
AGNs (All; $\lambda_E \leq 0.1$ )	$-0.92 \pm 0.90$	$-0.41 \pm 0.04$	$0.33 \pm 0.06$
AGNs (All; $\lambda_E > 0.1$ )	$-4.72 \pm 0.04$	$-0.58^a$	$0.33 \pm 0.06$
AGNs (All; $\lambda_E > 0.1$ )	$-2.21 \pm 0.43$	$-0.45 \pm 0.02$	$0.23 \pm 0.06$
Inactive (E+CB)	$-2.01 \pm 0.63$	$-0.50 \pm 0.03$	$0.31 \pm 0.03$
AGNs (E+CB)	$-2.71 \pm 0.06$	$-0.50^a$	$0.39 \pm 0.05$
AGNs (E+CB)	$-1.72 \pm 1.19$	$-0.45 \pm 0.05$	$0.39 \pm 0.05$
AGNs (E+CB; $\lambda_E \leq 0.1$ )	$-1.71 \pm 0.08$	$-0.45^a$	$0.41 \pm 0.07$
AGNs (E+CB; $\lambda_E > 0.1$ )	$-2.02 \pm 0.08$	$-0.45^a$	$0.23 \pm 0.09$
Inactive (PB)	$-2.72 \pm 0.14$	$-0.50^a$	$0.63 \pm 0.09$
AGNs (PB)	$-3.02 \pm 0.05$	$-0.50^a$	$0.24 \pm 0.07$
AGNs (PB)	$-2.12 \pm 0.05$	$-0.45^a$	$0.22 \pm 0.07$
AGNs (PB; $\lambda_E \leq 0.1$ )	$-1.89 \pm 0.09$	$-0.45^a$	$0.30 \pm 0.13$
AGNs (PB; $\lambda_E > 0.1$ )	$-2.20 \pm 0.05$	$-0.45^a$	$0.13 \pm 0.07$

<sup>a</sup>The slope is fixed for the fit.

Note. — Col. (1): Sample;  $\lambda_E \equiv L_{\text{bol}}/L_{\text{Edd}}$ ; “E” = ellipticals; “CB” = classical bulges; “PB” = pseudo bulges. Col. (2): Zero point of the  $M_{\text{BH}}-M_{R,\text{bul}}$  relation. Col. (3): Slope of the  $M_{\text{BH}}-M_{R,\text{bul}}$  relation. Col. (4): Intrinsic scatter of the  $M_{\text{BH}}-M_{R,\text{bul}}$  relation.

to their bulge type, as given in Kormendy & Ho (2013). The fit for ellipticals and classical bulges yields  $\alpha = -2.01 \pm 0.63$ ,  $\beta = -0.50 \pm 0.03$  and  $\epsilon_0 = 0.31 \pm 0.03$ . Given that pseudo bulges are expected to exhibit much larger scatter (Kormendy & Ho 2013), we do not fit them independently and instead fix the slope of the correlation to that of ellipticals and classical bulges, solving only for its zero point. We find a zero point of  $\alpha = -2.72 \pm 0.14$ , indeed significantly lower than that of ellipticals and classical bulges (Figure 1; Table 1).

Figures 2 and 3 show the  $M_{\text{BH}}-L_{\text{bul}}$  relation for our type 1 AGN sample, using different assumptions to estimate the BH mass. As discussed in Section 2.2, the virial factor depends on the bulge type. In Figure 2, we simply adopt a single virial factor to estimate the BH mass, assuming that AGN hosts follow the same  $M_{\text{BH}}-\sigma_*$  relation of inactive galaxies regardless of bulge type. The best fit for the AGNs yields an  $M_{\text{BH}}-L_{\text{bul}}$  relation with  $\alpha = -2.27 \pm 0.40$ ,  $\beta = -0.46 \pm 0.02$  and  $\epsilon_0 = 0.36 \pm 0.04$ . Although the slope of the  $M_{\text{BH}}-L_{\text{bul}}$  relation of AGNs is slightly shallower than that of inactive galaxies, we caution against any physical interpretation of this result because our AGN sample is drawn from various heterogeneous *HST* programs. Differences in zero point may be more straightforward to assess. If we fix the slope of the relation to that of inactive galaxies, we find that the zero point of AGNs is systematically lower than that of inactive galaxies, by  $\sim 0.64$  dex in  $M_{\text{BH}}$  or  $\sim 1.10$  mag in  $M_{\text{bul}}$ .

To investigate the main driver of the offset between active and inactive galaxies in the  $M_{\text{BH}}-L_{\text{bul}}$  relation, we divide the sample into two subgroups according to Eddington ratio ( $\lambda_E \equiv L_{\text{bol}}/L_{\text{Edd}}$ ). We again find that the two subgroups clearly deviate in  $M_{\text{BH}}-L_{\text{bul}}$  space, in the sense that AGNs with higher

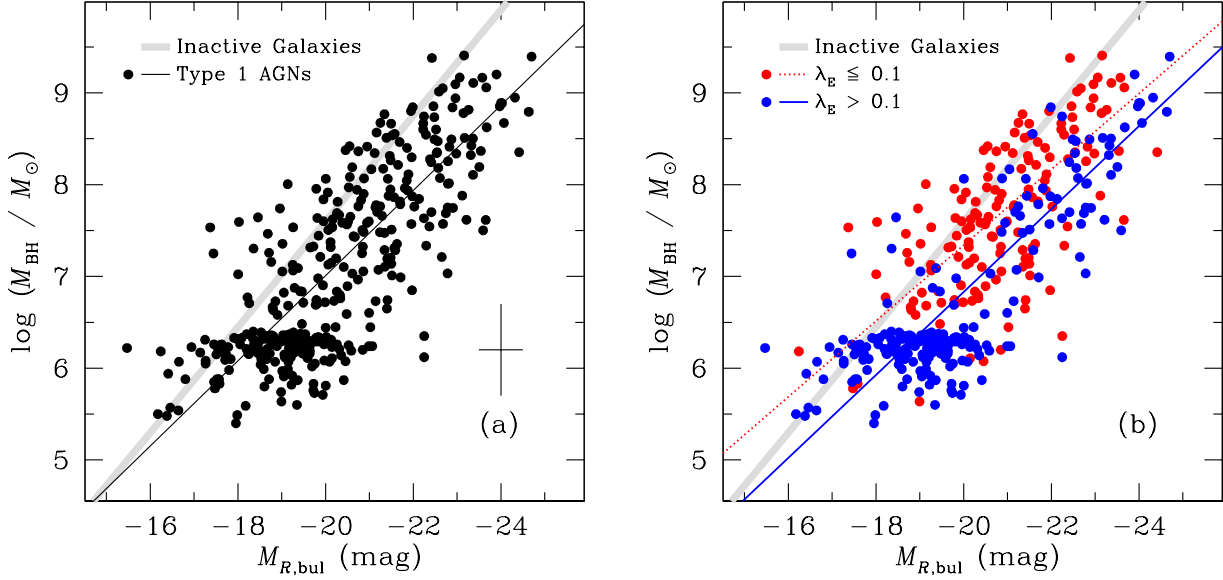


**Figure 2.** Correlation between BH mass and absolute  $R$ -band magnitude for the bulges of type 1 AGNs. Shaded grey line represents the relation for all inactive galaxies regardless of their bulge type (see Fig. 1). (a) Solid line gives the relation for the entire AGN sample, with BH mass estimated using a single virial factor regardless of bulge types. The typical uncertainties (0.5 dex in BH mass and 0.5 mag in bulge magnitude) are given in the lower-right corner. (b) The sample is divided according to accretion rate: red points and dotted line represent low Eddington ratio ( $\lambda_E \leq 0.1$ ); blue points and solid line denote high Eddington ratio ( $\lambda_E > 0.1$ ).

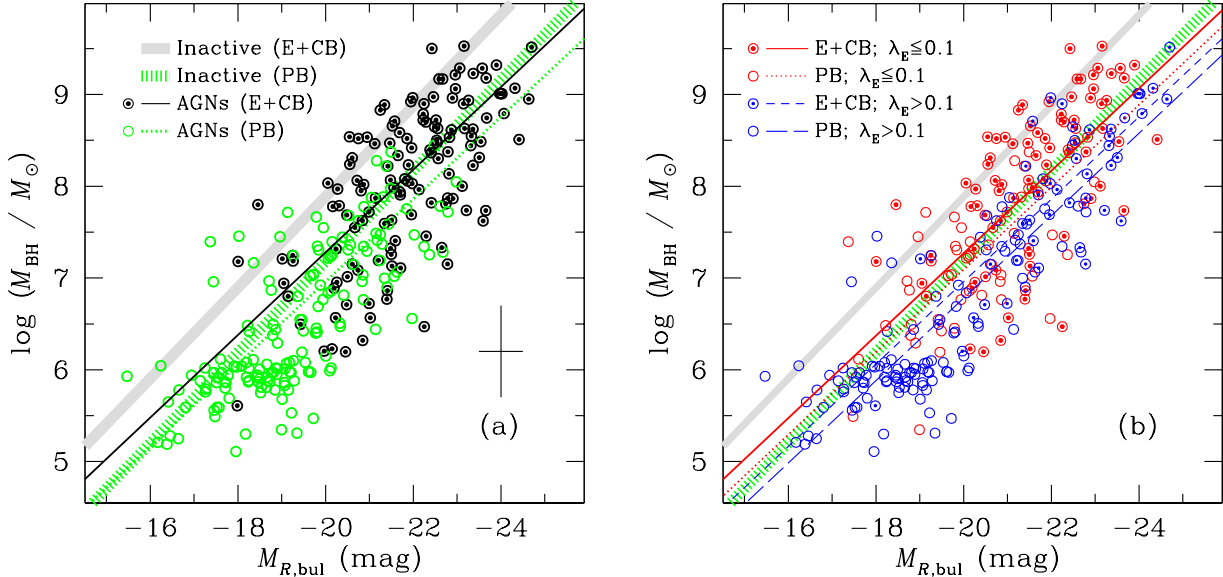


**Figure 3.** Same as Figure 2, except that the BH masses are estimated using different virial factors for pseudo bulges and classical bulges (Ho & Kim 2014). The shaded grey line represents the relation for inactive ellipticals and classical bulges from Kormendy & Ho (2013); the thick green dotted line denotes the relation for inactive pseudo bulges (see Section 3.1). (a) AGNs residing in ellipticals and classical bulges are represented by semi-filled circles and the solid line, while those hosted in pseudo bulges are represented by open circles and the dashed line. (b) The sample is further divided according to accretion rate and bulge type. Objects with low Eddington ratio ( $\lambda_E \leq 0.1$ ) hosted in ellipticals and classical bulges are plotted as semi-filled red circles and dotted line, while those in pseudo bulges are shown as open red circles and dotted line. Objects with high Eddington ratio ( $\lambda_E > 0.1$ ) hosted in ellipticals and classical bulges are plotted as semi-filled blue circles and solid line, while those in pseudo bulges are shown as open blue circles and solid line.

Eddington ratio ( $\lambda_E > 0.1$ <sup>5</sup>) tend to have lower BH mass of brighter bulge (Figure 2b).

To properly account for the fact that the  $M_{\text{BH}} - \sigma_*$  relation depends on bulge type, Figure 3 reexamines the correlation using BH masses calculated according to host galaxy bulge type. As for the inactive galaxies, we fix the slope of the relation of AGNs with pseudo bulges to that of AGNs with

ellipticals and classical bulges. At a given bulge luminosity, the BH masses of AGNs are significantly smaller than those of inactive galaxies; alternatively, at fixed BH mass AGNs have more luminous bulges than non-AGNs. For a quantitative comparison, we fix the slope of the relation to that of inactive ellipticals and classical bulges ( $\beta = -0.50 \pm 0.03$ ). The zero point of the  $M_{\text{BH}} - L_{\text{bul}}$  relation for the AGN sample ( $\alpha = -2.71 \pm 0.06$  for ellipticals and classical bulges;  $\alpha = -3.02 \pm 0.05$  for pseudo bulges) is significantly lower

<sup>5</sup> We adopt this criterion because it is the median value of the sample

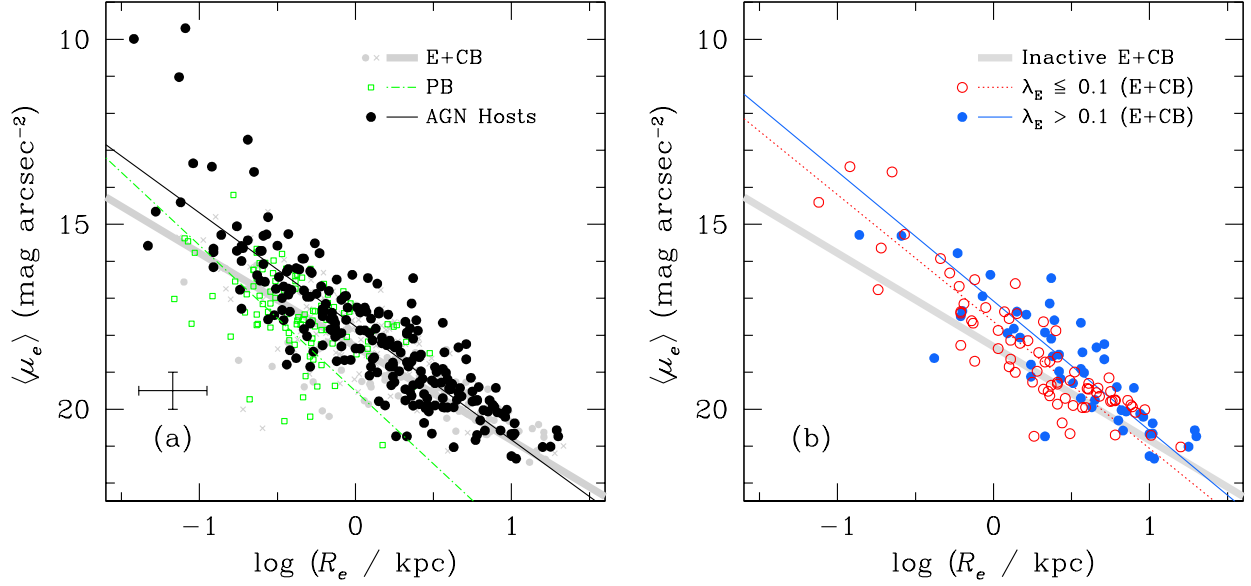


**Figure 4.** Correlation between effective radius  $R_e$  and mean surface brightness  $\langle \mu_e \rangle$  at  $R_e$  (the Kormendy relation) for the bulges of AGN host galaxies. (a) The filled circles and solid line represent host galaxies of AGNs irrespective of their bulge type. For the comparison with inactive galaxies, we overplot the elliptical galaxies from Bender et al. (1992), Gadotti (2009), and Kormendy et al. (2009) (grey circles), disk galaxies with classical bulges from Bender et al. (1992), Fisher & Drory (2008), Gadotti (2009), and Laurikainen et al. (2010) (grey crosses), and disk galaxies with pseudo bulges from Fisher & Drory (2008), Gadotti (2009), and Laurikainen et al. (2010) (green squares). The relation for the inactive ellipticals and classical bulges is denoted by the grey line, while that for inactive pseudo bulges is denoted by the green dashed-dotted line. The typical uncertainties (0.5 mag in  $\langle \mu_e \rangle$  and  $\sim 0.2$  in  $\log R_e$ ) for active galaxies are given in the lower-left corner. (b) Here we only highlight the ellipticals and classical bulges, and divide the AGN hosts by Eddington ratio. The Kormendy relation for inactive galaxies is shown by the grey line. AGNs with low Eddington ratio are plotted as in red circles and red dotted line; those with high Eddington ratio are plotted in blue filled circles and blue solid line.

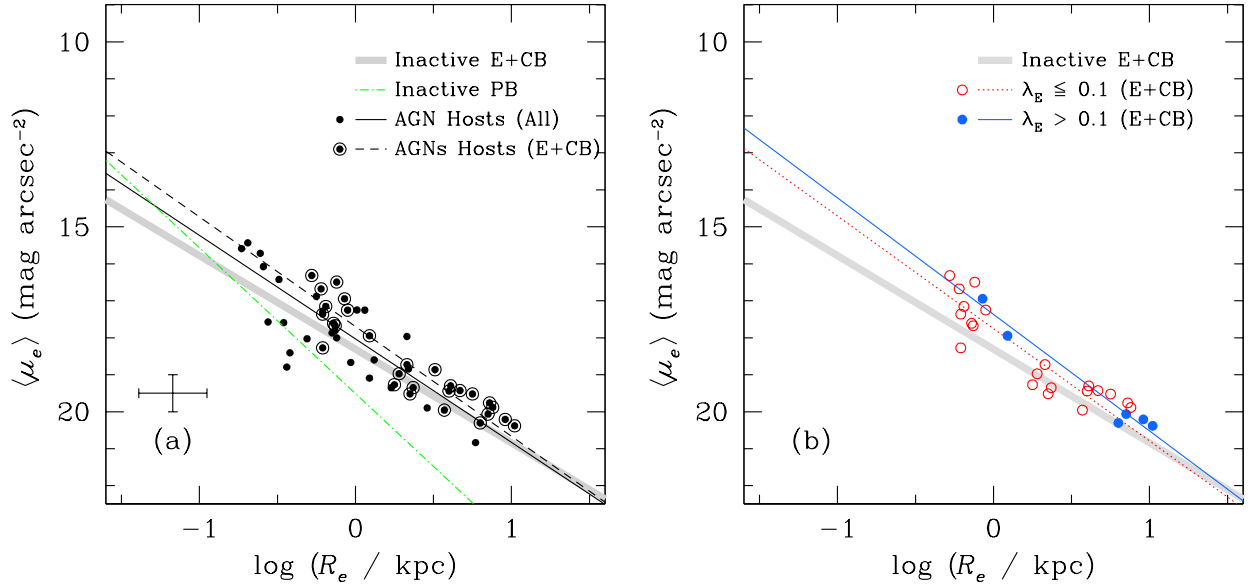


**Figure 5.** Same as Figure 4, except that we only plot AGN hosts with the most reliable measurements of bulge properties.

than those of inactive galaxies ( $\alpha = -2.01 \pm 0.63$  for ellipticals and classical bulges;  $\alpha = -2.72 \pm 0.14$  for pseudo bulges). It is interesting to note that the degree of the offset is larger for classical bulges ( $\Delta\alpha \approx 0.7$ ) compared to pseudo bulges ( $\Delta\alpha \approx 0.3$ ).

### 3.2. Kormendy Relation

The interpretation of the observed offset between active and inactive galaxies in the  $M_{\text{BH}} - L_{\text{bul}}$  relation is ambiguous. Do AGNs have undermassive BHs or overluminous bulges? Here we introduce another diagnostic that can break the degener-

acy, one that strongly favors the possibility that active galaxies have overluminous bulges. We make use of the empirical inverse correlation between bulge effective radius ( $R_e$ ) and mean effective surface brightness ( $\langle \mu_e \rangle$ ) obeyed by normal galaxies. Kormendy's (1977) relation was first introduced to study the bulges of early-type and S0 galaxies. Figure 4 shows the Kormendy relation for our AGN sample and for a sample of inactive galaxies assembled from the literature. The relation is derived using the ordinary least-squares bisector, which considers  $R_e$  and  $\langle \mu_e \rangle$  as independent variables. For a proper comparison between active and inactive galaxies, measure-

Table 2. Kormendy Relation for Different Subsamples ( $\langle\mu_e\rangle = \alpha + \beta \log(R_e/\text{kpc})$ )

Subsamples (1)	$\alpha$ (2)	$\beta$ (3)
Inactive (E+CB)	$18.31 \pm 0.03$	$2.53 \pm 0.06$
Inactive (PB)	$19.51 \pm 0.09$	$3.94 \pm 0.29$
AGNs (All)	$17.76 \pm 0.06$	$3.07 \pm 0.11$
AGNs (E+CB; $\lambda_E \leq 0.1$ )	$17.63 \pm 0.11$	$3.43 \pm 0.22$
AGNs (E+CB; $\lambda_E > 0.1$ )	$17.08 \pm 0.22$	$3.50 \pm 0.31$
AGNs (E+CB; $\lambda_E \leq 0.1$ ) <sup>a</sup>	$17.75 \pm 0.14$	$3.04 \pm 0.29$
AGNs (E+CB; $\lambda_E > 0.1$ ) <sup>a</sup>	$17.38 \pm 0.16$	$3.15 \pm 0.22$

<sup>a</sup>AGN hosts with reliable measurements of photometric properties of bulges.

Note. — Col. (1): Sample;  $\lambda_E \equiv L_{\text{bol}}/L_{\text{Edd}}$ ; “E” = ellipticals; “CB” = classical bulges; “PB” = pseudo bulges. Col. (2): Zero point of the Kormendy relation. Col. (3): Slope of the Kormendy relation.

ment errors in  $\langle\mu_e\rangle$  and  $R_e$  are not taken into account during the fit, as those values are uncertain for inactive galaxies. It appears, at first sight, that active galaxies follow a tight relation systematically offset toward higher surface brightness relative to inactive galaxies. Three objects (Fairall 9, [HB89] 1549+203, and HE 0054–2239) have exceptionally compact bulges ( $R_e < 0.1$  kpc). As the apparent  $R_e$  of these outliers are comparable to the size of the point-spread function ( $\sim 0''.1$ ), we deem their size measurements to be suspicious and exclude them from further consideration.

We also overplot bulge measurements for nearby inactive galaxies drawn from a variety of sources (Bender et al. 1992; Fisher & Drory 2008; Gadotti 2009; Kormendy et al. 2009; Laurikainen et al. 2010). To estimate  $R$ -band surface brightness, we apply optical color conversions according to morphological types from Fukugita et al. (1995) (e.g.,  $B-R = 1.57$  and  $V-R = 0.61$  for ellipticals;  $B-R = 1.39$  and  $V-R = 0.53$  for S0s). For the  $K$ -band data from Laurikainen et al. (2010), we adopt  $R-K = 2.56$  for S0/Sa galaxies using the template spectral energy distributions of Polletta et al. (2007). For Sloan Digital Sky Survey galaxies (Gadotti 2009), we adopt the conversions from Ivezić et al. (2007). Note that the control sample of inactive galaxies is contaminated by low-luminosity AGNs (e.g., Gadotti 2009). However, AGN bolometric luminosity of low-luminosity AGNs ( $\sim 10^{43}$  erg s<sup>-1</sup>) in the control sample of inactive galaxies inferred from a median [O III] luminosity are significantly lower than that of our sample of type 1 AGNs ( $\sim 10^{44.5}$  erg s<sup>-1</sup>). As a sanity check, we test if those low-luminosity AGNs affect the Kormendy relation of inactive galaxies by performing the fits with and without low-luminosity AGNs, and find that the change in the Kormendy relation is negligible.

It is still unclear whether the Kormendy relation depends on bulge type (Gadotti 2009; but see Laurikainen et al. 2010; Gao et al. 2018). Following standard convention (e.g., Kormendy & Kennicutt 2004; Fisher & Drory 2008), we divide the sample of inactive disk galaxies into two classes according to their bulge Sérsic index: classical bulges ( $n > 2$ ) and pseudo bulges ( $n \leq 2$ ). Classical bulges follow a trend very similar to that of elliptical galaxies, while pseudo bulges tend to have a fainter zero point, larger scatter, and a seemingly steeper slope. As the origin of the difference between the two bulge types is beyond the scope of this study, we here only focus on the Kormendy relation of ellipticals and clas-

sical bulges, whose intrinsic tightness provides a more useful reference for comparison with the AGN sample (Figure 4b). Whereas our AGN hosts appear to follow a similar Kormendy relation as inactive galaxies, active galaxies tend to be systematically overluminous (higher  $\langle\mu_e\rangle$ ) compared to inactive early-type galaxies (ellipticals and classical bulges). The differences become most pronounced at  $R_e \leq 3$  kpc. The systematic deviation of AGN host galaxies from the Kormendy relation of normal, early-type galaxies is reminiscent of the behavior of ultraluminous infrared galaxies and quasars (Rothberg et al. 2013), here reaffirmed with a larger sample. We also find that the degree of luminosity offset depends on accretion rate, in the sense that AGNs with higher Eddington ratio tend to have systematically higher effective surface brightness.

The complexity of the image decomposition of AGNs prompts us to examine whether systematic measurements errors or biases may artificially induce the apparent differences between active and inactive galaxies. To test this hypothesis, we discard objects whose fits may have been compromised by a high nucleus-to-bulge luminosity ratio, small  $R_e$ , strong morphological disturbance, point-spread function mismatch, inadequate field-of-view of the image, and dust obscuration. The Kormendy relation of the remaining subset of 58 objects, for which the errors in  $\langle\mu_e\rangle$  and  $R_e$  are less than 0.5 mag and 0.2 dex, respectively, are plotted in Figure 5. Although the slope and zero point have changed from the previous result for the entire sample, the results are qualitatively similar: AGN host galaxies have brighter bulges than inactive galaxies. Table 2 summarizes the fits of the Kormendy relation for the various subsamples discussed above.

## 4. DISCUSSION

### 4.1. The Origin of Overluminous Bulges

Our analysis provides two lines of evidence—one based on the  $M_{\text{BH}} - L_{\text{bul}}$  relation and the other on the size-surface brightness (Kormendy) relation—that the host galaxies of type 1 AGNs possess bulges that deviate from those of inactive galaxies of similar size and morphological type. Moreover, the degree of departure from inactive galaxies increases systematically with increasing Eddington ratio of the AGN.

Taken by itself, the systematic offset between active and inactive galaxies on the  $M_{\text{BH}} - L_{\text{bul}}$  relation lends itself to multiple interpretations. One possibility is that active galaxies possess undermassive BHs relative to inactive galaxies of the same bulge luminosity. The effect would be substantial for the current sample, amounting to  $\sim 0.3 - 0.7$  dex in  $M_{\text{BH}}$ . Indeed, a very similar but less extreme effect was noted by Kim et al. (2008b), who, investigating a more limited sample of low-redshift quasar host galaxies, argued that accretion rate is one of the primary parameters responsible for the scatter in the  $M_{\text{BH}} - L_{\text{bul}}$  relation. Ho & Kim (2014), too, reported qualitatively similar results for a subset of 44 reverberation-mapped AGNs with sufficient *HST* imaging to decompose the bulges of the host galaxies. Luminous type 1 AGNs trace actively growing BHs, and it is plausible that they might possess undermassive BHs that will eventually “catch up” to the  $M_{\text{BH}} - L_{\text{bul}}$  relation of inactive galaxies at the end of the AGN phase, provided, of course, that BH accretion systematically lags behind bulge growth. Our sample has a median  $\lambda_E \approx 0.1$ . Assuming that these BHs grow with a constant accretion rate of  $0.1\lambda_E$  during a typical AGN lifetime of  $\sim 100$  Myr (Martini 2004), a radiative efficiency of  $\epsilon = 0.1$  would imply a very



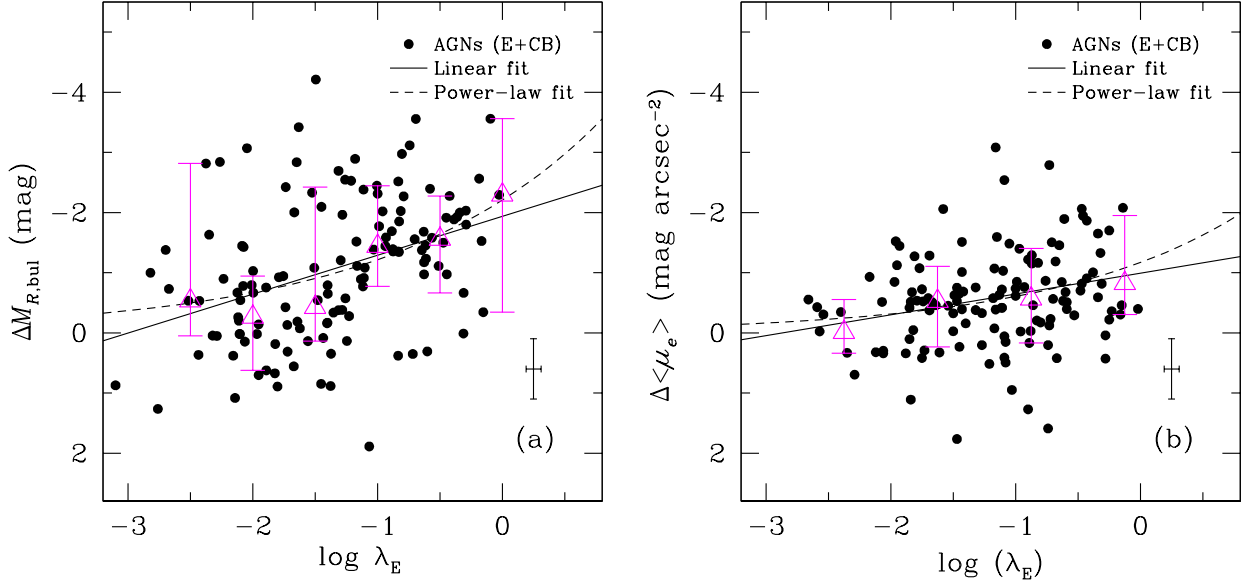


**Figure 6.** Dependence of excess bulge brightness on Eddington ratio ( $\lambda_E$ ). The typical uncertainties (0.5 mag in  $\Delta M_{R,\text{bul}}$  and  $\langle \mu_e \rangle$  and  $\sim 0.06$  dex in  $\lambda_E$  are given in the lower-right corner. (a) The amount of excess bulge luminosity ( $\Delta M_{R,\text{bul}}$ ) represents the difference between the measured  $M_{\text{bul}}$  and that inferred from the  $M_{\text{BH}}-M_{\text{bul}}$  relation of inactive galaxies. (b) The amount of excess in mean surface brightness represents the difference between the measured  $\langle \mu_e \rangle$  and that inferred from the Kormendy relation of inactive ellipticals and classical bulges. For both panels, the solid line indicates a linear fit, and the dashed line denotes a power-law fit. The magenta triangles represent the median value in each bin, and error bars enclose the central 68% of the values.

modest BH mass increase of only  $\sim 0.1$  dex. The growth rate can be even smaller because the accretion rate of type 1 AGNs might decrease with time (Kelly et al. 2010), or the AGN lifetime may be shorter than 100 Myr (Martini 2004). This falls far short of explaining the magnitude of the observed offset.

Alternatively, we might posit that the BH masses suffer from some unknown systematic bias that caused them to be underestimated. This seems highly implausible because the BH masses were estimated using a virial mass estimator whose virial factor was derived under the explicit assumption that reverberation-mapped AGNs obey the  $M_{\text{BH}}-\sigma_*$  relation of inactive galaxies. Ho & Kim (2014) did note that the virial factor may depend on Eddington ratio, but the effect is mild ( $\sim 0.2$  dex). In any event, the reverberation-mapped AGNs used by Ho & Kim (2014) to calibrate the virial factor have a median  $\lambda_E = 0.07$ , essentially identical to that of the current sample (median  $\lambda_E = 0.1$ ).

The third and in our view most natural explanation is that AGN host galaxies possess *overluminous* bulges, primarily as a consequence of recent star formation. For our current sample, the amount of brightening is  $\sim 0.6 - 1.4$  mag in the  $R$  band. This interpretation is entirely consistent with previous studies that find that AGNs are often associated with young stellar populations (Kauffmann et al. 2003; Nelson et al. 2004; Letawe et al. 2010; Trump et al. 2013; Lutz et al. 2018). Letawe et al. (2010) showed that the host galaxies of nearby quasars tend to have colors typical of starbursts or late-type galaxies. The host galaxies of the local sample of reverberation-mapped AGNs, too, appear to be brighter than normal galaxies at a given velocity dispersion (Nelson et al. 2004), a conclusion since confirmed by Ho & Kim (2014) based on detailed analysis of their bulge component. In principle, the bulge brightness of AGN hosts can also be enhanced by contamination from extended, narrow emission-line regions. To quantify this effect, we adopt the equivalent widths of [O III]  $\lambda 5007$  of type 2 quasars, the strongest emission line observed in these sys-

tems (Zakamska et al. 2003), which should serve as a conservative upper limit for type 1 AGNs. Taking into account the FWHM of the filter response functions of typical *HST* broad-band filters (1500–2500 Å), the observed equivalent widths of [O III] in type 2 quasars imply that extended narrow-line emission contributes less than 0.03 mag to our broad-band photometry of the host galaxy bulge. This should be regarded as a strict upper limit because type 2 quasars on average have higher Eddington ratios ( $\langle \lambda_E \rangle \approx 0.2$ ; Kong & Ho 2018) than our sample ( $\langle \lambda_E \rangle \approx 0.1$ ). Thus, emission-line contamination cannot explain to the excess brightness observed in the host galaxy bulges.

Our analysis of the Kormendy relation of AGN host galaxies provides powerful, independent evidence that their bulges have enhanced brightness. Unlike the  $M_{\text{BH}}-L_{\text{bul}}$  relation, the Kormendy relation does not suffer from ambiguities regarding the BH mass. The bulges of AGN host galaxies populate a Kormendy relation that sits systematically *above* that of normal, inactive galaxies. At a given  $R_e$ , the bulges of AGNs have brighter  $\langle \mu_e \rangle$ , and the effect is stronger at small  $R_e$ . It is difficult to imagine that bulge size is the main driver for the systematic offset, because the size evolution of bulges is negligible for the low redshifts of our sample (e.g., Trujillo et al. 2011). Thus, it is natural to suppose that surface brightness is enhanced in the bulges of AGN hosts, and the physical origin for the luminosity increase must be recent star formation. Zhao et al. (2019) independently arrived at the same conclusion for a sample of low-redshift type 2 quasars.

For more quantitative discussion, we estimate the enhancement of the bulge brightness in AGN hosts compared to normal galaxies, both in the  $M_{\text{BH}}-L_{\text{bul}}$  relation and Kormendy relation. We define  $\Delta M_{\text{bul}} \equiv M_{R,\text{bul}} - M_{R,\text{bul}}(M_{\text{BH}})$  as the difference between the measured bulge luminosity and the bulge luminosity predicted from the BH mass based on the  $M_{\text{BH}}-L_{\text{bul}}$  relation of inactive galaxies. Similarly,  $\Delta \langle \mu_e \rangle \equiv \langle \mu_e \rangle - \langle \mu_e \rangle(R_e)$  is the difference between the observed mean effective surface brightness and that expected from the Kor-

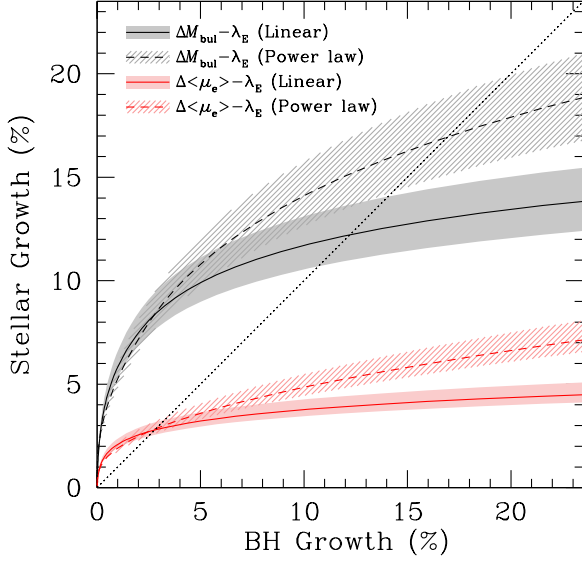


**Figure 7.** Comparison between BH growth rate and stellar growth rate inferred from Figure 6. For the BH growth rate, we assume that the AGN lifetime is 50 Myr and that the Eddington ratio is constant over this period. For the stellar growth rate, we assume that the SFR is constant over a star formation lifetime of 500 Myr, and that young stars have  $[\text{Fe}/\text{H}] = 0$ . The relation derived from the  $\Delta M_{\text{bul}} - \lambda_E$  relation is shown as black lines, while that derived from the  $\Delta \langle \mu_e \rangle - \lambda_E$  relation is shown as red lines, both for the linear and power-law fits. The shaded regions represent the error budget due to the unknown metallicity of the young stellar population. The adopted  $[\text{Fe}/\text{H}]$  ranges from  $-2.3$  to  $0.7$ . The dotted line represents the case where the BH growth rate is identical to the stellar growth rate.

mendy relation of inactive galaxies. We examine the dependence of  $\Delta M_{\text{bul}}$  and  $\Delta \langle \mu_e \rangle$  on accretion rate, restricting our attention only to the subset of hosts that are ellipticals and classical bulges. The large intrinsic scatter of pseudo bulges in both scaling relations precludes any meaningful conclusions to be drawn for this type of bulges. Figure 6a shows that the accretion rate is significantly correlated with  $\Delta M_{\text{bul}}$ . We estimate a Spearman correlation coefficient of  $\rho = -0.43$  and a probability of  $P_{\text{null}} < 10^{-4}$  for the hypothesis of no correlation. The correlation between accretion rate and  $\Delta \langle \mu_e \rangle$  is somewhat weaker, but still statistically significant ( $\rho = -0.22$  and  $P_{\text{null}} \approx 0.01$ ). An ordinary least squares linear fit yields  $\Delta M_{\text{bul}} = -0.65 - 1.94 \log \lambda_E$  and  $\Delta \langle \mu_e \rangle = -0.99 - 0.35 \log \lambda_E$ . It is intriguing that the fit for  $\Delta M_{\text{bul}}$  is steeper than that for  $\Delta \langle \mu_e \rangle$ , suggesting that the excess of bulge brightness is higher in the  $M_{\text{BH}} - L_{\text{bul}}$  relation than in the Kormendy relation. We caution, however, as discussed above, that systematic uncertainties in BH mass measurements may introduce additional sources of scatter in the  $M_{\text{BH}} - L_{\text{bul}}$  relation. A power-law model may provide a better description of the data than a linear model. We find  $\Delta M_{\text{bul}} = -2.2 \lambda_E^{0.26}$  and  $\langle \mu_e \rangle = -1.2 \lambda_E^{0.29}$ . The overall trends are similar for both fits, judging by the similarity of their root mean square deviation (RMSD). For  $\Delta M_{\text{bul}}$ , RMSD = 21.5 for the linear fit and 21.7 for the power-law fit; for  $\Delta \langle \mu_e \rangle$ , the corresponding values are RMSD = 9.3 and 9.3, respectively.

#### 4.2. Implications for the Coevolution of BHs and Their Host Galaxies

The dependence of excess bulge brightness on Eddington ratio suggests that star formation activity increases with increasing BH accretion rate. This is naturally expected from

the strong correlations between BH and bulge properties (Kormendy & Ho 2013), which have long been interpreted as evidence of a close physical connection between BH and galaxy growth, or BH accretion rate and SFR. We employ a simple toy model to investigate how BH growth and stellar growth in the host galaxy are synchronized. Assuming that the excess bulge light arises primarily from young stars, we naturally expect that the degree of excess increases with increasing  $f_{\text{young}}$ , the ratio of young to old stars, which is equivalent to the stellar growth rate. In order words, the light excess is zero if the bulge contains only old stars (i.e.  $f_{\text{young}} = 0$ ). To estimate the stellar growth rate, we assume that the age of the old stellar population in ellipticals and classical bulges is 10 Gyr (e.g., Zoccali et al. 2003; Brown et al. 2006), and that recent star formation occurs with a constant SFR over the duration of the star formation phase. The lifetime of the star formation phase is difficult to constrain, as it can span a wide range (100 Myr to a few Gyr) and depends on the origin of star formation activity (e.g., Kennicutt 1998; Tacconi et al. 2006; Hickox et al. 2012). For simplicity, we assume a star formation lifetime of 500 Myr, but our conclusions do not depend strongly on this choice. With these assumptions,

$$\text{stellar mass growth rate} \equiv f_{\text{young}} = \frac{M_{*, < 500 \text{ Myr}}}{M_{*, 10 \text{ Gyr}}} \times 100, \quad (4)$$

where  $M_{*, < 500 \text{ Myr}}$  and  $M_{*, 10 \text{ Gyr}}$  are the stellar masses of the young and old populations, respectively. We employ a simple stellar population model from Bruzual & Charlot (2003) to calculate the mass-to-light ( $M/L$ ) ratio in the  $R$  band, and derive the relation between  $M/L$  and  $f_{\text{young}}$ . Finally, we convert the excess bulge brightness ( $\Delta M_{\text{bul}}$  and  $\Delta \langle \mu_e \rangle$ ) to  $f_{\text{young}}$ . Our fiducial model assumes that both old and young stars have solar metallicity, but we explore the effect of varying metallicity on  $M/L$ , denoted by the shaded regions in Figure 7.

Assuming that the Eddington ratio is constant over the lifetime of the AGN, the BH growth ratio can be expressed as  $\exp\left(\lambda_E \frac{1-\epsilon}{\epsilon} \frac{t_{\text{AGN}}}{t_{\text{Edd}}}\right)$ , where  $\epsilon = 0.1$  is the assumed radiative efficiency,  $t_{\text{AGN}} = 0.05$  Gyr is the assumed lifetime of the AGN<sup>6</sup>, and  $t_{\text{Edd}}$  is the Eddington timescale ( $= 0.45$  Gyr), defined as  $M_{\text{BH}} c^2 / L_{\text{Edd}}$  (Volonteri & Rees 2005). Our main conclusions do not depend sensitively to these adopted values.

Figure 7 shows the results of this simple toy model, comparing the BH growth rate and stellar growth rate in AGN hosts as inferred from the fitted relations from Figure 6. As expected, the two quantities are clearly correlated. The absolute ratio between the stellar growth rate and BH growth rate has no physical meaning because it can depend strongly on our assumptions for the input parameters (e.g., lifetimes and radiative efficiency). Interestingly, the slope of the relation (i.e. ratio of stellar growth rate to BH growth rate) decreases mildly with increasing BH growth rate (i.e. accretion rate). Although it is unclear what causes this gradual change, this finding suggests that the *recent* specific SFR is non-linearly correlated with the Eddington ratio of the AGN. It may also be consistent with the notion that star formation can be suppressed by AGN activity (e.g., AGN outflows; Di Matteo et al. 2005). The strength of AGN outflows is expected to be proportional to the accretion rate (e.g., Ciccone et al. 2014).

<sup>6</sup> The actual AGN lifetime is somewhat uncertain (10–100 Myr; Martini 2004).



## 5. SUMMARY

Using a new compendium of photometric parameters of the host galaxies of nearby type 1 AGNs, we show that the bulges of the host galaxies are overluminous ( $\sim 1$  mag in the  $R$  band) compared to those of inactive galaxies. The effect becomes more pronounced with increasing accretion rate. This is revealed both in the  $M_{\text{BH}} - L_{\text{bul}}$  relation and in the bulge size-surface brightness (Kormendy) relation. We argue that the excess bulge brightness in AGN hosts most likely reflects their young stellar population, an interpretation consistent with previous, independent studies based on optical colors or spectra. Our methodology, which relies solely on photometric decomposition and analysis of high-resolution images of the host galaxy in a single optical filter, demonstrates that the  $M_{\text{BH}} - L_{\text{bul}}$  and Kormendy relations are powerful tools to probe the physical connection between supermassive BHs and their host galaxies. We present a simple toy model to illustrate the positive correlation between the stellar growth rate of the host galaxy and the growth rate of the BH. The relative growth rate of stellar mass and BH mass decreases with increasing Eddington ratio, a possible manifestation of star formation suppression by AGN feedback.

We are grateful to an anonymous referee for very constructive comments. This work was supported by the National Key Program for Science and Technology Research and Development (2016YFA0400702), the National Science Foundation of China (11721303), and the National Research Foundation of Korea (NRF) grant funded by the Korea government (MSIP) (No. 2017R1C1B2002879). We made use of the NASA/IPAC Extragalactic Database (NED), which is operated by the Jet Propulsion Laboratory, California Institute of Technology, under contract with NASA.

## REFERENCES

- Alonso-Herrero, A., Ramos Almeida, C., Esquej, P., et al. 2014, *MNRAS*, 443, 2766
- Bender, R., Burstein, D., & Faber, S. M. 1992, *ApJ*, 399, 462
- Bessell, M. S. 2005, *ARA&A*, 43, 293
- Bettoni, D., Falomo, R., Kotilainen, J. K., Karhunen, K., & Uslenghi, M. 2015, *MNRAS*, 454, 4103
- Brown, T. M., Smith, E., Ferguson, H. C., et al. 2006, *ApJ*, 652, 323
- Bruce, V. A., Dunlop, J. S., Mortlock, A., et al. 2016, *MNRAS*, 458, 2391
- Bruzual, G., & Charlot, S. 2003, *MNRAS*, 344, 1000
- Calzetti, D., Kinney, A. L., & Storchi-Bergmann, T. 1994, *ApJ*, 429, 582
- Canalizo, G., & Stockton, A. 2013, *ApJ*, 772, 132
- Cardamone, C. N., Urry, C. M., Schawinski, K., et al. 2010, *ApJL*, 721, L38
- Cicone, C., Maiolino, R., Sturm, E., et al. 2014, *A&A*, 562, A21
- Collin, S., Kawaguchi, T., Peterson, B. M., & Vestergaard, M. 2006, *A&A*, 456, 75
- Di Matteo, T., Springel, V., & Hernquist, L. 2005, *Natur*, 433, 604
- Fisher, D. B., & Drory, N. 2008, *AJ*, 136, 773
- Fukugita, M., Shimasaku, K., & Ichikawa, T. 1995, *PASP*, 107, 945
- Gadotti, D. A. 2009, *MNRAS*, 393, 1531
- Gao, H., Ho, L. C., Barth, A. J., & Li, Z.-Y. 2018, *ApJ*, 862, 100
- . 2019, arXiv e-prints, arXiv:1901.03195
- Hickox, R. C., Mullaney, J. R., Alexander, D. M., et al. 2014, *ApJ*, 782, 9
- Hickox, R. C., Wardlow, J. L., Smail, I., et al. 2012, *MNRAS*, 421, 284
- Ho, L. C. 2005, *ApJ*, 629, 680
- Ho, L. C., Filippenko, A. V., & Sargent, W. L. W. 2003, *ApJ*, 583, 159
- Ho, L. C., & Kim, M. 2009, *ApJS*, 184, 398
- . 2014, *ApJ*, 789, 17
- Into, T., & Portinari, L. 2013, *MNRAS*, 430, 2715
- Ivezić, Ž., Smith, J. A., Miknaitis, G., et al. 2007, *AJ*, 134, 973
- Jiang, Y.-F., Greene, J. E., Ho, L. C., Xiao, T., & Barth, A. J. 2011, *ApJ*, 742, 68
- Kaspi, S., Smith, P. S., Netzer, H., et al. 2000, *ApJ*, 533, 631
- Kauffmann, G., Heckman, T. M., Tremonti, C., et al. 2003, *MNRAS*, 346, 1055
- Kelly, B. C., Vestergaard, M., Fan, X., et al. 2010, *ApJ*, 719, 1315
- Kennicutt, Jr., R. C. 1998, *ARA&A*, 36, 189
- Kim, M., Ho, L. C., & Im, M. 2006, *ApJ*, 642, 702
- Kim, M., Ho, L. C., Peng, C. Y., Barth, A. J., & Im, M. 2008a, *ApJS*, 179, 283
- . 2017, *ApJS*, 232, 21
- Kim, M., Ho, L. C., Peng, C. Y., et al. 2008b, *ApJ*, 687, 767
- Kinney, A. L., Calzetti, D., Bohlin, R. C., et al. 1996, *ApJ*, 467, 38
- Kong, M., & Ho, L. C. 2018, *ApJ*, 859, 116
- Kormendy, J., Fisher, D. B., Cornell, M. E., & Bender, R. 2009, *ApJS*, 182, 216
- Kormendy, J., & Ho, L. C. 2013, *ARA&A*, 51, 511
- Krawczyk, C. M., Richards, G. T., Mehta, S. S., et al. 2013, *ApJS*, 206, 4
- Laurikainen, E., Salo, H., Buta, R., Knapen, J. H., & Comerón, S. 2010, *MNRAS*, 405, 1089
- Letawe, Y., Letawe, G., & Magain, P. 2010, *MNRAS*, 403, 2088
- Lutz, D., Shimizu, T., Davies, R. I., et al. 2018, *A&A*, 609, A9
- Magorrian, J., Tremaine, S., Richstone, D., et al. 1998, *AJ*, 115, 2285
- Martini, P. 2004, *Coevolution of Black Holes and Galaxies*, 169
- Matsuoka, Y., Strauss, M. A., Price, III, T. N., & DiDonato, M. S. 2014, *ApJ*, 780, 162
- McLure, R. J., & Dunlop, J. S. 2004, *MNRAS*, 352, 1390
- Mullaney, J. R., Pannella, M., Daddi, E., et al. 2012, *MNRAS*, 419, 95
- Nelson, C. H., Green, R. F., Bower, G., Gebhardt, K., & Weistrop, D. 2004, *ApJ*, 615, 652
- Netzer, H. 2009, *MNRAS*, 399, 1907
- Nolan, L. A., Dunlop, J. S., Kukulka, M. J., et al. 2001, *MNRAS*, 323, 308
- O'Dowd, M. J., Schiminovich, D., Johnson, B. D., et al. 2009, *ApJ*, 705, 885
- Onken, C. A., Ferrarese, L., Merritt, D., et al. 2004, *ApJ*, 615, 645
- Peng, C. Y., Ho, L. C., Impey, C. D., & Rix, H.-W. 2002, *AJ*, 124, 266
- . 2010, *AJ*, 139, 2097
- Peng, C. Y., Impey, C. D., Ho, L. C., Barton, E. J., & Rix, H.-W. 2006, *ApJ*, 640, 114
- Planck Collaboration, Ade, P. A. R., Aghanim, N., et al. 2016, *A&A*, 594, A13
- Polletta, M., Tajer, M., Maraschi, L., et al. 2007, *ApJ*, 663, 81
- Rosario, D. J., Santini, P., Lutz, D., et al. 2012, *A&A*, 545, A45
- Rosario, D. J., Mozena, M., Wuyts, S., et al. 2013, *ApJ*, 763, 59
- Rosario, D. J., McIntosh, D. H., van der Wel, A., et al. 2015, *A&A*, 573, A85
- Rothberg, B., Fischer, J., Rodrigues, M., & Sanders, D. B. 2013, *ApJ*, 767, 72
- Sánchez, S. F., Jahnke, K., Wisotzki, L., et al. 2004, *ApJ*, 614, 586
- Schawinski, K., Virani, S., Simmons, B., et al. 2009, *ApJL*, 692, L19
- Shangguan, J., Ho, L. C., & Xie, Y. 2018, *ApJ*, 854, 158
- Shi, Y., Ogle, P., Rieke, G. H., et al. 2007, *ApJ*, 669, 841
- Shipley, H. V., Papovich, C., Rieke, G. H., et al. 2013, *ApJ*, 769, 75
- Silverman, J. D., Mainieri, V., Lehmer, B. D., et al. 2008, *ApJ*, 675, 1025
- Symeonidis, M. 2017, *MNRAS*, 465, 1401
- Symeonidis, M., Giblin, B. M., Page, M. J., et al. 2016, *MNRAS*, 459, 257
- Tacconi, L. J., Neri, R., Chapman, S. C., et al. 2006, *ApJ*, 640, 228
- Tremaine, S., Gebhardt, K., Bender, R., et al. 2002, *ApJ*, 574, 740
- Treu, T., Stiavelli, M., Casertano, S., Möller, P., & Bertin, G. 2002, *ApJL*, 564, L13
- Trujillo, I., Ferreras, I., & de La Rosa, I. G. 2011, *MNRAS*, 415, 3903
- Trump, J. R., Hsu, A. D., Fang, J. J., et al. 2013, *ApJ*, 763, 133
- Volonteri, M., & Rees, M. J. 2005, *ApJ*, 633, 624
- Woo, J.-H., Treu, T., Barth, A. J., et al. 2010, *ApJ*, 716, 269
- Zakamska, N. L., Strauss, M. A., Krolik, J. H., et al. 2003, *AJ*, 126, 2125
- Zhao, D., Ho, L. C., Zhao, Y., Shanguan, Z., & Kim, M. 2019, submitted
- Zoccali, M., Renzini, A., Ortolani, S., et al. 2003, *A&A*, 399, 931